Identification of a Novel Prognosis-Associated ceRNA Network in Lung Adenocarcinoma via Bioinformatics analysis

Yumiao Li
Hebei University
Xiaoxue Yu
Hebei University
Yuhao Zhang
Hebei University
Xiaofang Wang
Hebei University
Linshan Zhao
Hebei University
Dan Liu
Hebei University
Guofa Zhao
Hebei University
Xiangpeng Gao
Hebei University
Jiejun Fu
Guangxi Medical University
Aimin Zang
Hebei University
Youchao Jia (youchaojia@163.com)
Hebei University https://orcid.org/0000-0001-9191-5836

Research

Keywords: Lung adenocarcinoma, LncRNAs, CeRNA, Biomarker, Prognosis

Posted Date: August 31st, 2021

DOI: https://doi.org/10.21203/rs.3.rs-845661/v1

Version of Record: A version of this preprint was published at BioMedical Engineering OnLine on November 24th, 2021. See the published version at https://doi.org/10.1186/s12938-021-00952-x.

Abstract

Backgroud: Long noncoding RNAs (lncRNAs) play an important role in the occurrence and development of lung adenocarcinoma (LUAD). The purpose of this study was to identify novel abnormally regulated lncRNA-microRNA (miRNA)-messenger RNA (mRNA) competing endogenous RNA (ceRNA) networks related to LUAD prognosis.

Methods: We programmed an Agilent Microarray Scanner to screen for differentially expressed (DE) lncRNAs and mRNAs in 4 paired LUAD samples. Gene Ontology (GO) and Kyoto Encyclopedia of Genes and Genomes (KEGG) pathway analyses were performed to annotate the DE lncRNAs and mRNAs. R bioinformatics packages, The Cancer Genome Atlas (TCGA) LUAD database and a Kaplan-Meier (KM) survival analysis tools were used to validate the microarray data and construct the lncRNA-miRNA-mRNA ceRNA regulatory network. Then, quantitative real-time PCR was used to validate the DE lncRNAs in 7 LUAD cell lines.

Results: A total of 2819 DE lncRNAs and 2396 DE mRNAs (*P*-value < 0.05 and fold change ≥2 or ≤0.5) were identified in 4 paired LUAD tissue samples. In total, 255 of these DE lncRNAs were also identified in TCGA. The GO and KEGG analysis results suggested that the DE genes were most enriched in angiogenesis and cell proliferation and closely related to human cancers. Moreover, the differential expression of ENST00000609697, ENST00000602992, and NR_024321 was consistent with the microarray data, as determined by quantitative real-time PCR validation in 7 LUAD cell lines, but only ENST00000609697 was associated with the overall survival of LUAD patients (log-rank *P*=0.029). Finally, through analysis of ENST00000609697 target genes, we identified the ENST00000609697–hsa-miR-6791-5p–RASL12 ceRNA network, which may play a tumor-suppressive role in LUAD.

Conclusion: ENST00000609697 was abnormally expressed in LUAD. Furthermore, downregulation of ENST00000609697 and its target gene RASL12 were associated with poor prognosis in LUAD. The ENST00000609697–hsa-miR-6791-5p–RASL12 axis may play a tumor-suppressive role. These results may suggest new prognostic and therapeutic biomarkers for LUAD.

Introduction

Lung cancer is the second most commonly diagnosed cancer worldwide, with 2.21 million new cases annually, but is the most common cause of cancer death (1.79 million deaths annually)[1]. Approximately 85% of lung cancer cases are non-small cell lung cancer (NSCLC), and lung adenocarcinoma (LUAD) is currently the most common histological subtype of NSCLC[2–4]. At diagnosis, some patients already have late-stage disease with poor prognosis. Early prevention and the continuous modernization of targeted drugs promotes clinical translation of the lung cancer treatment model, prolongs the progression-free survival (PFS) and overall survival (OS) of patients, and improves their prognosis[5]. However, the 5-year survival rate of lung cancer is still low (4–17%). Therefore, the prediction and exploration of biomarkers for early diagnosis and therapeutic targets in LUAD is a very urgent need.

Long noncoding RNAs (LncRNAs) are noncoding RNA (ncRNA) molecules more than 200 nucleotides in length that are most commonly not translated into proteins and are crucial players in diverse cellular and physiological functions[6, 7]. Recently, with the development and application of high-throughput sequencing and gene chip technologies, researchers have found that lncRNAs play an important role in the occurrence and development of a variety of tumors[8]. lncRNAs abnormally expressed in tumor tissues not only can be used as specific tumor biomarkers for early diagnosis and prognosis but also can directly interact with DNA, messenger RNA (mRNA) or protein molecules to regulate chromatin modification or structural changes or to affect gene transcription, splicing and translation[9]. In general, lncRNAs can regulate a variety of physiological and pathological processes in tumor development, such as cell proliferation, differentiation, migration, and invasion; stem cell reprogramming; tumorigenesis; and drug resistance[10–14]. However, the discovery of new functional lncRNAs in LUAD is lacking. Therefore, identifying more lncRNAs related to LUAD diagnosis and prognosis is a worthwhile endeavor.

Competing endogenous RNAs (ceRNAs) are RNAs containing microRNA (miRNA) recognition elements (MREs)[15]. They can regulate the expression of genes harboring the corresponding MRE or the expression of proteins by competitively binding to miRNAs[16]. LncRNAs can also act as ceRNAs, which play a role in the formation of lncRNA-miRNA-mRNA ceRNA networks[16, 17]. Aberrant expression of ceRNAs promotes dysregulation of the ceRNA regulatory network and is related to the biological processes of tumor cell proliferation, apoptosis, growth, invasion, migration and metastasis[17]. Perturbation of ceRNA networks could affect diseases and may explain disease processes and present opportunities for new therapies[16]. For instance, multiple studies have demonstrated that in various cancers, patients with high HOTAIR expression exhibit higher lymphatic invasion and shorter survival times[18–23]. Studies have shown that HOTAIR acts as a ceRNA for miR-331-3p to regulate the HER2 expression level, promoting the tumorigenesis of gastric cancer cells[24]. HOTAIR has also been shown to competitively bind to miR-193a to upregulate the expression of c-KIT, facilitating acute myeloid leukemia (AML) progression[25]. Moreover, linc01234 was found to be upregulated in gastric cancer. It can competitively bind miR-204-5p, promote CBFB gene expression, and then promote the occurrence of gastric cancer. However, knockdown of linc01234 in vitro increased the expression of miR-204-5p, decreased the gene expression of CBFB, and significantly inhibited cell proliferation and invasion[26].

In this study, we used gene chip technology to screen LUAD tissue samples and analyzed and predicted the multiple crucial functions of the identified differentially expressed (DE) lncRNAs and DE mRNAs. Our results revealed novel lncRNA-miRNA-mRNA ceRNA regulatory networks, which may contain new specific therapeutic targets and pathways related to LUAD survival.

Results

Identification of DE lncRNAs and mRNAs in lung adenocarcinoma and adjacent tissues

In our study, microarray profiling performed with 4 paired LUAD tissue samples (tumor and paracarcinoma tissues) to identify DE lncRNAs and DE mRNAs. An overview of this study is shown in Fig. 1. In general, we identified 2819 lncRNAs and 2396 mRNAs with significant differential expression (*P*-value < 0.05 and fold change (FC) ≥ 2 or ≤ 0.5): 859 upregulated lncRNAs and 1960 downregulated lncRNAs; 757 upregulated and 1639 downregulated mRNAs. The hierarchical clustering heatmap showed the expression levels of the DE lncRNAs (Fig. 2A) and mRNAs (Fig. 2B) and distinguished cancer from adjacent tissues based on the molecular signature of these DE lncRNAs and mRNAs. By volcano plot and scatter plot analyses evaluating the overall distribution of the two sets of data, these DE RNAs were divided into up- and downregulated lncRNAs (Fig. 2C) and up- and downregulated mRNAs (Fig. 2D). The number of downregulated genes was significantly greater than that of upregulated genes. In addition, the top 20 significantly DE lncRNAs and mRNAs were identified according to FC values and are shown in Tables 1 and 2.

Table 1
Top-20 differentially expressed lncRNAs of lung adenocarcinoma and adjacent tissue samples

Accession	pvalues	FC(abs)	Regulation	Chr	GeneSymbol
ENST00000423781	0.045138791	154.273527	up	chr7	AC004870.4
lnc-SYT16-1:1	0.008110801	62.1498876	up	chr14	—
lnc-TSPAN13-2:1	0.000027973	34.927184	up	chr7	—
ENST00000431027	0.007829215	26.7528941	up	chr1	RP3-340N1.2
NR_046533	0.000809301	25.2378211	up	chr13	CLDN10-AS1
lnc-BCKDHB-4:1	0.002525077	18.4268214	up	chr6	—
ENST00000605886	0.04382729	16.6142073	up	chr1	RP11-284F21.10
NR_125404	0.023786704	15.962481	up	chr3	LOC100505920
lnc-USP26-3:1	0.003316762	15.7760352	up	chrX	—
lnc-BCKDHB-6:1	0.006763185	13.5382121	up	chr6	—
lnc-NSRP1-2:2	0.000161724	27.71072711	down	chr17	—
ENST00000480831	0.001737636	15.74807358	down	chr3	ADAMTS9-AS1
ENST00000432452	0.001497719	14.60031376	down	chr10	RP11-464C19.3
lnc-GTDC1-15:1	0.000686192	14.54798755	down	chr2	—
ENST00000443224	0.000787963	14.36781879	down	chr10	RP11-371A19.2
lnc-ZPLD1-2:2	0.004414129	14.01720412	down	chr3	—
ENST00000507525	0.000368778	13.3686819	down	chr4	RP13-577H12.2
lnc-TRAPPC5-1:1	0.001126285	12.74950409	down	chr19	—
NR_003928	0.012408513	12.17016938	down	chr1	CHIAP2
ENST00000624132	0.015263542	11.88176057	down	chr9	RP11-205K6.3

Table 2
Top-20 differentially expressed mRNA of lung adenocarcinoma and adjacent tissue samples

Accession	pvalues	FC(abs)	Regulation	Chr	GeneSymbol
NM_173076	0.00025142	112.2153919	up	chr2	ABCA12
NM_003695	0.02604819	93.23154863	up	chr8	LY6D
NM_001032280	0.01004802	63.89111709	up	chr6	TFAP2A
NM_032899	0.00605935	41.28293568	up	chr8	FAM83A
NM_001199042	0.03422378	40.11209326	up	chr15	STRA6
NM_001164431	0.01571357	38.51455003	up	chr20	ARHGAP40
NM_025153	0.00026241	35.86487577	up	chr5	ATP10B
NM_001080407	0.02410958	30.83360008	up	chr11	GLB1L3
NM_001251830	0.00046426	30.81333114	up	chr4	SPP1
NM_001077188	0.00251909	30.572041	up	chrX	HS6ST2
NM_012391	0.00602412	26.86301237	up	chr6	SPDEF
NM_001045	0.00033657	45.9038257	down	chr17	SLC6A4
NM_000261	0.000161133	30.0889688	down	chr1	MYOC
NM_001114133	0.00024818	20.6970509	down	chr10	SYNPO2L
NM_203451	0.000202297	19.3511029	down	chr13	SERTM1
NM_001332	0.000243926	16.3150335	down	chr5	CTNND2
NM_153370	0.000374892	15.9720912	down	chr6	PI16
NM_021146	0.005748437	15.6408757	down	chr1	ANGPTL7
NM_000575	0.000118471	14.9645892	down	chr2	IL1A
NM_001278236	0.003914533	14.8213111	down	chr11	PTPN5
NM_032961	0.000080895	14.6704759	down	chr4	PCDH10

Validation of the DE lncRNAs via The Cancer Genome Atlas (TCGA) database

To verify the microarray data in a large cohort of clinical samples, we downloaded the TCGA LUAD database, which contains both gene expression and patient survival data for the screened cohort, and obtained 573 samples (including 514 LUAD tissue samples and 59 adjacent tissue samples). The clinical information of the patients is shown in Table 3. As shown in the hierarchical clustering heatmap (Fig. 2E) and the volcano plot (Fig. 2F), 1916 DE lncRNAs (| log2FC| > 1, $P < 0.05$), namely, 1271 upregulated and 645 downregulated lncRNAs, were identified. As shown in the Venn diagram (Fig. 2G), the intersection of

the 2819 DE lncRNAs identified by microarray analysis with the 1916 DE lncRNAs identified by TCGA database analysis contained 255 overlapping DE lncRNAs.

Table 3
The Clinicopathological characteristics of LUAD samples downloaded from TCGA database.

Clinicopathological characteristics	Patients (N = 514)	
	N	%
Age		
< 68	280	54.4
≥ 68	224	43.6
Gender		
Male	240	46.7
Female	274	53.3
Pathologic stage		
Stage I	279	54.3
Stage II	122	23.7
Stage III	78	15.2
Stage V	26	2.5
Pathologic T		
T1	172	33.5
T2	277	53.9
T3	46	4.4
T4	18	1.7
Tx	4	< 0.3
Pathologic N		
NO	335	32.5
N1	95	9.2
N2	68	6.6
N3	2	< 0.1
Pathologic M		
MO	340	33.0
M1	25	4.86

Clinicopathological characteristics	Patients (N = 514)	
	N	%
Mx	144	14.0
Vital status		
Alive	333	32.3
Dead	181	17.6

Annotation Analyses Of The De Lncrnas And Mrnas

GO analysis was used to annotate gene functions and standardize the descriptions of the DE genes according to the biological process (BP), cellular component (CC), and molecular function (MF) categories. We analyzed the results of cis-regulated lncRNAs and found that most of the top 30 GO terms enriched with the upregulated and downregulated genes (i.e., DE lncRNAs and DE mRNAs) were in the BP and CC categories (Fig. 3A, 3B). The top 3 descriptive terms enriched with the DE lncRNAs were atomic septum development, structural molecule activity conferring elasticity, and embryonic digestive tract morphogenesis (Fig. 3C). However, condensed chromosome outer kinetochore, cell migration involved in heart development, and regulation of vasculogenesis were the top 3 descriptive terms enriched with the DE mRNAs (Fig. 3D). Moreover, all DE lncRNAs and DE mRNAs were involved in angiogenesis and cell proliferation.

In our study, KEGG, a database for pathway analysis of DE genes to identify their biological functions, was divided into the following six classifications: cellular processing, environmental information processing, genetic information processing, human diseases, metabolism, and organismal systems. Comprehensive analysis of the KEGG classification results for the DE lncRNAs (Fig. 3G) and DE mRNAs (Fig. 3H) showed that the DE genes were enriched mainly in the signal transduction, immune system, and cancers: overview pathway terms. Moreover, KEGG pathway enrichment analysis suggested that the DE genes were enriched mainly in vascular smooth muscle contraction, focal adhesion and TGF beta signaling pathway (Fig. 3E, F). Further analysis of the KEGG pathway term human diseases showed that these genes were closely related to small cell lung cancer, NSCLC, melanoma, glioma, prostate cancer, thyroid cancer, colorectal cancer (CRC) and other tumors (Fig. 3G, H).

Analysis Of Lncrna Target Genes

To further clarify the functional annotations of the DE genes, we determined the intersection of the 1302 DE lncRNA target genes and the 2396 DE mRNAs. Then, 523 common DE genes were selected via Venn diagram software (Fig. 4A). GO analysis showed that these genes were also enriched in the CC and BP categories. Moreover, the main enriched terms were extracellular matrix, myosin complex, and

cytoskeleton in the CC category (Fig. 4B); signal transduction in the BP category (Fig. 4C); and peptidase activity in the MF category (Fig. 4D). The KEGG analysis results showed that these genes were enriched mainly in the pathways focal adhesion, axon guidance, differentiated cardiomyopathy, and melanoma (Fig. 4E). These results suggested that these genes may play an important role in cell morphology, adhesion, intercellular connections, and signal transduction.

Candidate DE lncRNA validation in LUAD cell lines and overall survival analysis

We selected 4 candidate DE lncRNAs from the 255 overlapping genes: 2 downregulated genes (ENST00000609697 and ENST00000443224) and 2 upregulated genes (ENST00000602992 and NR_024321). To confirm the screening results, the expression of the 4 DE lncRNAs was validated in 7 LUAD cell lines and compared with that in the BEAS-2B cell line using qRT-PCR (Fig. 5A). The expression of ENST00000609697 and ENST00000443224 showed a significant decreasing trend in almost all 7 LUAD cell lines, consistent with the microarray data ($P < 0.05$), while ENST00000443224 was upregulated in H1993 cells ($P < 0.05$) (Fig. 5A). The significant increasing trend ($P < 0.05$) in ENST00000602992 and NR_024321 expression was also consistent with the microarray data, but the increasing trend in NR_024321 expression was not obvious in H2228 cells (Fig. 5B). Furthermore, we downloaded gene expression data and patient follow-up data from the TCGA dataset to further elucidate whether these candidate genes are potential prognostic markers for LUAD. Through TCGA dataset analysis, we found that ENST00000609697 was downregulated ($P < 0.001$) (Fig. 5C) and was the only candidate gene related to the prognosis of LUAD (log-rank $P = 0.029$) (Fig. 5D). ENST00000602992 and NR_024321 were upregulated in the TCGA dataset ($P < 0.001$) (Figure S1A, S1B). However, ENST00000602992 was not associated with the prognosis of LUAD ($P = 0.24$) (Figure S1C), and upregulation of NR_024321 was not positively correlated with good prognosis in LUAD ($P = 0.018$) (Figure S1D). Moreover, downregulation of ENST00000609697 was positively correlated with good prognosis in LUAD. It was considered the candidate biomarker and may act as a tumor suppressor.

Cerna Regulatory Network Of The De Lncrnas

To further illustrate the potential interactions among the DE lncRNAs, DE miRNAs and DE mRNAs involved in LUAD, lncRNA-miRNA-mRNA ceRNA networks were constructed, and a total of 188 DE lncRNAs, 444 DE miRNAs and 410 DE mRNAs were selected (Supplement S1E). Moreover, we found that most DE lncRNAs in the ceRNA regulatory network were downregulated. We singled out the ceRNA network of the candidate gene ENST00000609697 and found that 7 miRNAs (hsa-miR-3191-3p, hsa-miR-4731-5p, hsa-miR-598-5p, hsa-miR-6791-5p, hsa-miR-4292, hsa-miR-4446-3p and hsa-miR-1827) and 20 DE mRNAs (COLGALT2, MYOCD, TNS1, RASL12, CNN1, and so on) are involved in this network (Fig. 6A). Hsa-miR-4731-5p was enriched and targeted most DE mRNAs in the ENST00000609697 ceRNA network, indicating that it may play a critical role in LUAD.

Functional and survival analyses considering the target DE mRNAs in the ENST00000609697 ceRNA network

Furthermore, we conducted GO enrichment analysis of the 20 targeted DE mRNAs in three ontologies: BP, CC and MF. The 30 GO terms most enriched with the 20 targeted DE mRNAs are shown in Fig. 6B. The most enriched GO terms in the BP, CC, and MF categories were smooth muscle cell differentiation, focal adhesion, and actin binding, respectively (Fig. 6B). Most DE mRNAs were mapped to the BP category; thus, we generated a BP cnetplot that showed the DE mRNAs associated with the top 10 BP terms, in which 4 DE mRNAs (CNN1, FLNC, FOXF1, and MYOCD) were enriched (Fig. 6C). FOXF1 and MYOCD are related to multiple biological processes, suggesting that they may be the critical genes in LUAD. The BP emaplot showed the overlapping relationship between each pair of terms (Fig. 6D) and suggested that smooth muscle cell differentiation was a very important biological process. For screening ceRNA networks related to the prognosis of LUAD, we downloaded the expression and survival data related to the 20 target DE mRNAs in the ENST00000609697 ceRNA network in the UCSC Xena database. The expression of RASL12 was downregulated in LUAD ($P < 0.0001$) (Fig. 6E), and downregulation of RASL12 was positively correlated with good prognosis ($P = 0.034$) (Fig. 6F). These results suggested that the ENST00000609697–hsa-miR-6791-5p–RASL12 axis may play a tumor-suppressive role in LUAD.

Discussion

Here, we identified 2819 DE lncRNAs and 2396 DE mRNAs, among which were 859 upregulated and 1960 downregulated lncRNAs and 757 upregulated and 1639 downregulated mRNAs. Far more genes were downregulated than upregulated, indicating that the downregulated genes may play an important role in the biological process of LUAD. To explore the potential mechanisms of the DE genes, we performed GO and KEGG analyses of the aberrantly expressed lncRNAs and mRNAs. GO analysis showed that the DE lncRNAs were enriched mainly in atomic septum development, structural molecule activity conferring elasticity, and embryonic digestive tract morphogenesis and that the DE mRNAs were enriched mainly in condensed chromosome outer kinetochore, cell migration involved in heart development, and regulation of vasculogenesis. However, all of the DE lncRNAs and DE mRNAs were involved in angiogenesis and cell proliferation. Abnormalities in these two processes are closely related to the occurrence and development of cancers[27, 28]. The KEGG classification results for the DE lncRNAs and DE mRNAs showed that they were enriched mainly in signal transduction, the immune system, and cancers. Moreover, KEGG pathway enrichment analysis suggested that these DE genes were enriched mainly in vascular smooth muscle contraction, focal adhesion and TGF beta signaling pathway. They were also closely related to small cell lung cancer, NSCLC, melanoma, glioma, prostate cancer, thyroid cancer, CRC and other cancers. According to a previous study, the focal adhesion and TGF beta signaling pathways play essential roles in cell proliferation, and dysregulation of these two pathways is closely associated with oncogenesis[29, 30]. In addition, to further verify whether the functional annotations of the DE lncRNAs and DE mRNAs were basically consistent, we used Venn diagram software to intersect the DE lncRNA target genes and the DE mRNAs and found 523 overlapping genes, which were involved mainly in the extracellular matrix, myosin complex, cytoskeleton, signal transduction, and so on. Moreover, the KEGG analysis results showed that these genes were enriched mainly in the focal adhesion and melanoma pathways. The main functional annotations of the DE lncRNAs and DE mRNAs suggested that these genes may play

important roles in cell morphology, adhesion, intercellular connections, and signal transduction and are highly related to cancer. Thus, they are worthy of further analysis and verification.

An increasing number of aberrantly expressed lncRNAs are being identified as novel key regulators of the development of multiple human cancers[31, 32]. Aberrantly expressed lncRNAs may serve as biomarkers or function as oncogenes or tumor suppressors[31]; however, most studies have focused on lncRNAs acting as oncogenes. For instance, Song et al. reported that the protein claudin-4 encoded by the CLDN4 gene was upregulated in gastric cancer and related to poor prognosis[33]. The expression levels of the lncRNAs CCAT1 and CCAT2 were found to be significantly increased in CRC, and both were significantly correlated with poor relapse-free survival (RFS) and overall survival; these lncRNAs could thus be used independently or jointly as important prognostic biomarkers in CRC[34]. In addition, lncTCF7 was found to be significantly overexpressed in liver tumor tissues and liver cancer stem cells (CSCs) and could recruit the SWI/SNF complex to the promoter of the TCF7 gene to regulate its expression, thus activating the Wnt signaling pathway[35]. In our study, intersection of the 2819 DE lncRNAs identified by microarray analysis with the 1916 DE lncRNAs identified by TCGA database analysis revealed 255 overlapping DE lncRNAs: 161 downregulated and 94 upregulated lncRNAs. Then, we selected 4 candidate DE lncRNAs—2 downregulated genes (ENST00000609697 and ENST00000443224) and 2 upregulated genes (ENST00000602992 and NR_024321) —for validation in 7 LUAD cell lines. The expression of ENST00000609697, ENST00000602992 and NR_024321 was consistent with the microarray data. However, by analyzing the relative expression levels of the candidate genes and the associations of these genes with patient survival in the TCGA dataset, we found that ENST00000609697 was downregulated and was the only candidate gene positively correlated with good prognosis in LUAD. Therefore, we considered it a candidate gene and hypothesized that it may be a novel tumor suppressor.

Recent studies revealed that lncRNAs can act as ceRNAs, competitively binding to miRNAs, to form lncRNA-miRNA-mRNA ceRNA networks and in turn play a critical role in the diagnosis, prognosis and treatment of cancer[17, 36]. For example, lncRNA-KRTAP5-AS1 and lncRNA-TUBB2A can competitively bind miR-596 and miR-3620-3p as ceRNAs to promote the expression of CLDN4, enhance cell proliferation and invasion, and promote epithelial–mesenchymal transition (EMT)[33]. To identify the potential interactions among the DE lncRNAs, DE miRNAs and DE mRNAs, we constructed lncRNA-miRNA-mRNA ceRNA networks, which contained a total of 188 DE lncRNAs, 444 DE miRNAs and 410 DE mRNAs. Interestingly, most of the DE lncRNAs in the ceRNA regulatory network were downregulated. We then screened the ENST00000609697 ceRNA network, which was downregulated and positively correlated with good prognosis in LUAD. This network contained 7 miRNAs (hsa-miR-3191-3p, hsa-miR-4731-5p, hsa-miR-598-5p, hsa-miR-6791-5p, hsa-miR-4292, hsa-miR-4446-3p and hsa-miR-1827) and 20 DE mRNAs (COLGALT2, MYOCD, TNS1, RASL12, CNN1, and so on). We performed in-depth analysis of the functions related to the ENST00000609697 ceRNA network and found that the most enriched GO terms in the BP, CC, and MF categories were smooth muscle cell differentiation, focal adhesion, and actin binding, respectively. Smooth muscle cell differentiation is very important for the stability and repair of the vascular system, and abnormalities in this biological process can directly or indirectly affect the growth, proliferation and migration of tumor cells and the tumor immune microenvironment[37–40].

Focal adhesions are the main center of cellular mechanical sensation and serve as the bridge between integrin, the extracellular matrix and the cytoskeleton, which is correlated with the tumor microenvironment. Changes in signal transmission through focal adhesions of malignant cells is very important for the metastasis of tumor cells[40–42]. However, actin binding-related proteins participate in the formation of the cytoskeleton and regulate cell adhesion and migration[43]. The proliferation, migration, and invasion of tumor cells are dependent on proteins related to angiogenesis, focal adhesions, and actin binding. Therefore, the ENST00000609697 ceRNA network may play an important role in the tumor microenvironment of LUAD, and its functions are worthy of further exploration.

Subsequently, we downloaded the expression and survival data of the 20 target DE mRNAs in the ENST00000609697 ceRNA network from the UCSC Xena database and found that the expression of RASL12 was downregulated in LUAD ($P < 0.0001$) and that RASL12 expression was positively correlated with good prognosis ($P = 0.034$). RASL12 is a member of the RAS-like GTPase family and is localized in the cytoplasm[44]. However, evidence that RASL12 plays a role as a small GTP-binding protein is lacking. However, studies have reported that RASL12 could be homologous with the RAS-like GTPases RERG, RASL11A, RASL11B, RASL10A and RASL10B, which play tumor-suppressive roles in human cancers[45–47]. In addition, a recent study reported that the tumor suppressor RASSF1 can form a complex with RASL12 and recruit RASL12 to microtubules[48]. Combining these findings with our results, we inferred that RASL12 may be a tumor suppressor and that the ENST00000609697–hsa-miR-6791-5p–RASL12 axis may play a tumor-suppressive role in LUAD. More experiments should be performed to verify the role and regulatory mechanism of this axis.

Conclusion

Our study identified DE lncRNAs and DE mRNAs in LUAD tissue samples via microarray profiling and bioinformatics analysis approaches. Our results showed that downregulation of ENST00000609697 and its target gene RASL12 was associated with poor prognosis in LUAD. We identified a novel ceRNA network (ENST00000609697–hsa-miR-6791-5p–RASL12) that might play a tumor-suppressive role. These results might indicate potential molecular therapeutic targets and biomarkers for LUAD.

Materials And Methods

Patient selection and tumor tissue collection

None of the patients with newly diagnosed lung adenocarcinoma received radiotherapy or chemotherapy before surgery. Lung adenocarcinoma tissues—both tumor and paracarcinoma (> 5 cm from the tumor) tissues—were obtained from patients during thoracic surgery at the Affiliated Hospital of Hebei University. Thirty-four pairs of tissue samples were collected and pathologically confirmed. We randomly selected 4 pairs of tissue samples for microarray screening: 4 tumor tissues (1-C, 5-C, 9-C, and 12-C) and 4 matched adjacent normal tissues (1-N, 5-N, 9-N, and 12-N). Information on the patients' characteristics is shown in Table 4. All tissue samples were kept in liquid nitrogen prior to RNA extraction.

Table 4
Summary of patient characteristics

Characteristic	Cancer Patients (n = 4)
Mean Age (years)	59
Sex	
Male	2
Female	2
Pathological Diagnosis	LUAD
pTNM Stage	
	0
	1
	3
	0

Cell Culture

The human bronchial epithelial cell line BEAS-2B and NSCLC cell lines (H1299, A549, H1975, HCC78, HCC827, H2228 and H1993) were purchased from the Typical Culture Preservation Commission Cell Bank of the Chinese Academy of Sciences (Shanghai, China) and showed no mycoplasma contamination. The BEAS-2B cell line was cultured in BEBM medium supplemented with bronchial epithelial cell growth factor (BEGM Kit, LONZA Corporation, USA). The NSCLC cell lines were cultured in RPMI 1640 medium (H1299, H1975, HCC78, HCC827, H2228 and H1993) or F12K medium (A549) supplemented with 10% fetal bovine serum and 1% penicillin–streptomycin and were incubated at 37°C in a humidified atmosphere containing 5% CO^2.

Total Rna Extraction And Quantitative Real-time Pcr (Qrt-pcr)

Total RNA was extracted from cells and tissues using TRIzol reagent (Invitrogen, USA) according to the manufacturer's instructions. First-strand cDNA was synthesized using a Revert Aid First Strand cDNA Synthesis Kit (Roche, USA). qRT-PCR for lncRNAs was performed in an Applied Biosystems 7500 Fast Real-Time PCR system (Applied Biosystems, USA) using One Step SYBR Prime Script (Roche, USA) according to the manufacturer's instructions. The primer sequences are shown in Table 5. The expression

levels of lncRNAs were normalized with reference to β-actin, and the relative lncRNA expression levels were calculated by the comparative ΔCt method.

Table 5
Primers used for qRT-PCR

Gene name	Forward primer (5'-3')	Reverse primer (5'-3')
ENST00000608161	AGCGTGTTCTCAGGAGCAGG	CACAGTTGCACAGACGACAGT
ENST00000609941	GGACAAGTGCTCAGAATTGCAT	CTTTTACTTAAGAGAATCTTTGCGGG
ENST00000609697	TGTGCTGTGTCCATCACCGA	TGATGCATTTATTACATTCCCAAAGCC
ENST00000443224	AGTGAAACTGTTGTCATCCTTAGTT	AGACAGTTCTAAACCAGACAATGACA
ENST00000602992	GACGCAGGGTGGTAGGGAAA	GGCTTCCCAGAGACACAAGC
ENST00000450016	CACTGCACTCCAGCTTGGGA	TTAATTTTTACAACAGCTTCCGGGGGA
NR-024321	TGGCTTGTCTTCCATCGTCC	GCACGAGGGTTGTTACAGGA
lnc-CDH1-5:1	CGGTCGGGTATGAGGCACAT	GCGCTGTGTGCATGTTGTTTG
β-Actin	CTCCTTAATGTCACGCACGAT	CATGTACGTTGCTATCCAGGC

Lncrna Microarray Analysis

Total RNA was amplified and labeled with a Low Input Quick Amp Labeling Kit, One-Color (Agilent Technologies, USA, Cat. #5190 – 2305), following the manufacturer's instructions. Labeled cRNA was purified with an RNeasy Mini Kit (QIAGEN, GmBH, Germany, Cat. #74106). Each slide was hybridized in a hybridization oven with 1.65 μg of Cy3-labeled cRNA using a Gene Expression Hybridization Kit (Agilent Technologies, USA, Cat. #5188–5242) according to the manufacturer's instructions. After 17 hours of hybridization, slides were washed in staining dishes with a Gene Expression Wash Buffer Kit (Agilent Technologies, USA, Cat. #5188–5327) following the manufacturer's instructions. Slides were scanned with an Agilent Microarray Scanner (Agilent Technologies, USA, Cat. #G2565CA) with default settings: dye channel, green; scan resolution, 3 μm; PMT. 100%; range, 20 bits. Data were extracted with Feature Extraction software 10.7 (Agilent Technologies, Santa Clara, CA, USA). Raw data were normalized with the quantile algorithm in the limma package in R.

Gene Ontology (GO) and Kyoto Encyclopedia of Genes and Genomes (KEGG) analyses

We performed GO enrichment (http://www.geneontology.org/) and KEGG pathway analysis (https://www.kegg.jp/). Fisher's exact test was used to identify enrichment, and the data were obtained with the R/Bioconductor package clusterProfiler with the following screening criteria: > = 2 DE genes in a certain term/GO category and a *P*-value < 0.05. The terms identified by the analysis were arranged in descending order according to the value of the enrichment factor, and the top 30 terms were considered.

Construction Of The Regulatory Network

To identify interactions among the differential lncRNAs and mRNAs, a coexpression network was constructed based on the normalized signal intensities of the DE genes. The miRNA-mRNA/lncRNA interactions were predicted by using miRanda (http://www.microrna.org/microrna/home.do). All mRNAs, lncRNAs and miRNAs were differentially expressed between the two groups. mRNA-lncRNAs coexpression was determined with a cutoff Pearson correlation coefficient (PCC) of 0.99 (only positive correlations were retained). Overlap of the same miRNA seed sequence binding site in a lncRNA-mRNA pair predicted a lncRNA-miRNA-mRNA ceRNA network. The lncRNA-miRNA-mRNA ceRNA network was constructed using Cytoscape software (The Cytoscape Consortium, San Diego, CA, USA).

Statistical analysis

All data are expressed as the mean ± standard error values. Paired sample comparisons were performed using unpaired two-tailed Student’s t-test. Multiple group comparisons were performed with one-way ANOVA followed by Dunnett's multiple comparison test. Statistical analyses were performed with GraphPad Prism 5 (GraphPad Software, USA). *P*-values less than 0.05 were considered to indicate statistically significant differences.

Abbreviations

lncRNAs
Long noncoding RNAs; LUAD:lung adenocarcinoma; ceRNA:competing endogenous RNA; DE:differentially expressed; GO:Gene Ontology; KEGG:Kyoto Encyclopedia of Genes and Genomes; KM:Kaplan-Meier; NSCLC:non-small cell lung cancer; PFS:progression-free survival; OS:overall survival; MREs:microRNA recognition elements; BP:biological process; CC:cellular component; MF:molecular function; AML:acute myeloid leukemia; CRC:colorectal cancer; PCC:Pearson correlation coefficient.

Declarations

Ethics approval and consent to participate

The study was approved by the clinical research ethics committee of the Affiliated Hospital of Hebei University, and all tissue samples were collected with the written informed consent of the patients.

Consent for publication

Not applicable.

Availability of data and materials

The datasets analyzed in this study are available from the corresponding authors on request.

Conflicts of interest

All authors declare that there are no conflicts of interest.

Funding

This study was supported by The Youth Scientific Research Fund Project of the Affiliated Hospital of Hebei University (grant number 2017Q002), The Key Scientific Research Fund Project of the Affiliated Hospital of Hebei University (grant number 2015Z005), The Hebei Province Government Foundation for Clinical Medical Talent Training and Basic Research Projects (grant number 361007), and The Outstanding Young Scientific Research and Innovation Team of Hebei University (grant number 605020521007).

Authors` contributions

YL: the development of project, data analysis and validation and manuscript writing. YX: sample collection. YJ and AZ: manuscript editing. Final approval of the manuscript submitted: all authors.

Acknowledgments

We thank for Shanghai Biotechnology Corporation for microarray profiling and bioinformatics analysis in the research.

References

1. Ferlay J, Colombet M, Soerjomataram I, Parkin DM, Piñeros M, Znaor A, et al: Cancer statistics for the year 2020: an overview. International Journal of Cancer 2020; n/a(n/a). DOI: https://doi.org/10.1002/ijc.33588.
2. Brahmer JR, Govindan R, Anders RA, Antonia SJ, Sagorsky S, Davies MJ, et al. The Society for Immunotherapy of Cancer consensus statement on immunotherapy for the treatment of non-small cell lung cancer (NSCLC). J Immunother Cancer. 2018;6(1):75. DOI:https://doi.org/10.1186/s40425-018-0382-2.
3. Liu Z, Sun D, Zhu Q, Liu X. The screening of immune-related biomarkers for prognosis of lung adenocarcinoma. Bioengineered. 2021;12(1):1273–85. DOI:https://doi.org/10.1080/21655979.2021.1911211.
4. Miyazawa T, Marushima H, Saji H, Kojima K, Hoshikawa M, Takagi M, et al. PD-L1 Expression in Non-Small-Cell Lung Cancer Including Various Adenocarcinoma Subtypes. Ann Thorac Cardiovasc Surg. 2019;25(1):1–9. DOI:https://doi.org/10.5761/atcs.oa.18-00163.
5. Lilian Zsákai A, Sipos J, Dobos, Dániel Erős, Csaba Szántai-Kis, Péter Bánhegyi et al: Targeted drug combination therapy design based on driver genes. Oncotarget 2019; 10(51):5255–5266. DOI: https://doi.org/10.18632/oncotarget.26985.

6. Ahmad M. Khalila b, Mitchell Guttmana c, Maite Huartea b, Manuel Garbera, Arjun Rajd, Dianali Rivea Moralesa b et al: Many human large intergenic noncoding RNAs associate with chromatin-modifying complexes and affect gene expression. PNAS 2009; 106(28):11667–11672. DOI: https://doi.org/10.1073/pnas.0904715106.
7. Guttman M, Amit I, Garber M, French C, Lin MF, Feldser D, et al. Chromatin signature reveals over a thousand highly conserved large non-coding RNAs in mammals. Nature. 2009;458(7235):223–7. DOI:https://doi.org/10.1038/nature07672.
8. Chi Y, Wang D, Wang J, Yu W, Yang J: Long Non-Coding RNA in the Pathogenesis of Cancers. Cells 2019; 8(9). DOI: https://doi.org/10.3390/cells8091015.
9. Bhan A, Mandal SS. LncRNA HOTAIR: A master regulator of chromatin dynamics and cancer. Biochim Biophys Acta. 2015;1856(1):151–64. DOI:https://doi.org/10.1016/j.bbcan.2015.07.001.
10. Bao Z, Yang Z, Huang Z, Zhou Y, Cui Q, Dong D. LncRNADisease 2.0: an updated database of long non-coding RNA-associated diseases. Nucleic Acids Res. 2019;47(D1):D1034–7. DOI:https://doi.org/10.1093/nar/gky905.
11. Geisler S, Coller J. RNA in unexpected places: long non-coding RNA functions in diverse cellular contexts. Nat Rev Mol Cell Biol. 2013;14(11):699–712. DOI:https://doi.org/10.1038/nrm3679.
12. Ponting CP, Oliver PL, Reik W. Evolution and functions of long noncoding RNAs. Cell. 2009;136(4):629–41. DOI:https://doi.org/10.1016/j.cell.2009.02.006.
13. Ye JR, Liu L, Zheng F. Long Noncoding RNA Bladder Cancer Associated Transcript 1 Promotes the Proliferation, Migration, and Invasion of Nonsmall Cell Lung Cancer Through Sponging miR-144. DNA Cell Biol. 2017;36(10):845–52. DOI:https://doi.org/10.1089/dna.2017.3854.
14. Bhan A, Soleimani M, Mandal SS. Long Noncoding RNA and Cancer: A New Paradigm. Cancer Res. 2017;77(15):3965–81. DOI:https://doi.org/10.1158/0008-5472.CAN-16-2634.
15. Fabian MR, Sonenberg N. The mechanics of miRNA-mediated gene silencing: a look under the hood of miRISC. Nat Struct Mol Biol. 2012;19(6):586–93. DOI:https://doi.org/10.1038/nsmb.2296.
16. Salmena L, Poliseno L, Tay Y, Kats L, Pandolfi PP. A ceRNA hypothesis: the Rosetta Stone of a hidden RNA language? Cell 2011; 146(3):353–358. DOI: https://doi.org/10.1016/j.cell.2011.07.014.
17. Zhao M, Feng J, Tang L. Competing endogenous RNAs in lung cancer. Cancer Biol Med. 2021;18(1):1–20. DOI:https://doi.org/10.20892/j.issn.2095-3941.2020.0203.
18. Ono H, Motoi N, Nagano H, Miyauchi E, Ushijima M, Matsuura M, et al. Long noncoding RNA HOTAIR is relevant to cellular proliferation, invasiveness, and clinical relapse in small-cell lung cancer. Cancer Med. 2014;3(3):632–42. DOI:https://doi.org/10.1002/cam4.220.
19. Xianghua Liu Z, Liu M, Sun J, Wang L, De Z. W: The long non-coding RNA HOTAIR indicates a poor prognosis and promotes metastasis in non-small cell lung cancer. Cancer Med 2014 3(3):632–642. DOI: https://doi.org/10.1002/cam4.220.
20. Ding C, Cheng S, Yang Z, Lv Z, Xiao H, Du C, et al. Long non-coding RNA HOTAIR promotes cell migration and invasion via down-regulation of RNA binding motif protein 38 in hepatocellular carcinoma cells. Int J Mol Sci. 2014;15(3):4060–76. DOI:https://doi.org/10.3390/ijms15034060.

21. Heubach J, Monsior J, Deenen R, Niegisch G, Szarvas T, Niedworok C, et al. The long noncoding RNA HOTAIR has tissue and cell type-dependent effects on HOX gene expression and phenotype of urothelial cancer cells. Mol Cancer. 2015;14:108. DOI:https://doi.org/10.1186/s12943-015-0371-8.
22. Kim K, Jutooru I, Chadalapaka G, Johnson G, Frank J, Burghardt R, et al. HOTAIR is a negative prognostic factor and exhibits pro-oncogenic activity in pancreatic cancer. Oncogene. 2013;32(13):1616–25. DOI:https://doi.org/10.1038/onc.2012.193.
23. Kogo R, Shimamura T, Mimori K, Kawahara K, Imoto S, Sudo T, et al. Long noncoding RNA HOTAIR regulates polycomb-dependent chromatin modification and is associated with poor prognosis in colorectal cancers. Cancer Res. 2011;71(20):6320–6. DOI:https://doi.org/10.1158/0008-5472.CAN-11-1021.
24. Liu XH, Sun M, Nie FQ, Ge YB, Zhang EB, Yin DD, et al. Lnc RNA HOTAIR functions as a competing endogenous RNA to regulate HER2 expression by sponging miR-331-3p in gastric cancer. Mol Cancer. 2014;13:92. DOI:https://doi.org/10.1186/1476-4598-13-92.
25. Xing CY, Hu XQ, Xie FY, Yu ZJ, Li HY, Bin Z, et al. Long non-coding RNA HOTAIR modulates c-KIT expression through sponging miR-193a in acute myeloid leukemia. FEBS Lett. 2015;589(15):1981–7. DOI:https://doi.org/10.1016/j.febslet.2015.04.061.
26. Chen X, Chen Z, Yu S, Nie F, Yan S, Ma P, et al. Long Noncoding RNA LINC01234 Functions as a Competing Endogenous RNA to Regulate CBFB Expression by Sponging miR-204-5p in Gastric Cancer. Clin Cancer Res. 2018;24(8):2002–14. DOI:https://doi.org/10.1158/1078-0432.Ccr-17-2376.
27. Otto T, Sicinski P. Cell cycle proteins as promising targets in cancer therapy. Nat Rev Cancer. 2017;17(2):93–115. DOI:https://doi.org/10.1038/nrc.2016.138.
28. Zhao Z, Sun W, Guo Z, Zhang J, Yu H, Liu B. Mechanisms of lncRNA/microRNA interactions in angiogenesis. Life Sci. 2020;254:116900. DOI:https://doi.org/10.1016/j.lfs.2019.116900.
29. Gough NR, Xiang X, Mishra L. TGF-beta Signaling in Liver, Pancreas, and Gastrointestinal Diseases and Cancer. Gastroenterology 2021. DOI: 10.1053/j.gastro.2021.04.064.
30. Mishra YG, Manavathi B. Focal adhesion dynamics in cellular function and disease. Cell Signal. 2021;85:110046. DOI:https://doi.org/10.1016/j.cellsig.2021.110046.
31. Zhang H, Chen Z, Wang X, Huang Z, He Z, Chen aY. Long non-coding RNA: a new player in cancer. JOURNAL OF HEMATOLOGY ONCOLOGY. 2013;6(37):1–7. DOI:https://doi.org/10.1186/1756-8722-6-37.
32. Kai-Xin L, Cheng C, Rui L, Zheng-Wei S, Wen-Wen T, Peng X. Roles of lncRNA MAGI2-AS3 in human cancers. Biomed Pharmacother. 2021;141:111812. DOI:https://doi.org/10.1016/j.biopha.2021.111812.
33. Song YX, Sun JX, Zhao JH, Yang YC, Shi JX, Wu ZH, et al. Non-coding RNAs participate in the regulatory network of CLDN4 via ceRNA mediated miRNA evasion. Nat Commun. 2021;12(1):3149. DOI:https://doi.org/10.1038/s41467-021-23211-y.
34. Ozawa T, Matsuyama T, Toiyama Y, Takahashi N, Ishikawa T, Uetake H, et al. CCAT1 and CCAT2 long noncoding RNAs, located within the 8q.24.21 'gene desert', serve as important prognostic biomarkers

in colorectal cancer. Ann Oncol. 2017;28(8):1882–8. DOI:https://doi.org/10.1093/annonc/mdx248.

35. Wang Y, He L, Du Y, Zhu P, Huang G, Luo J, et al. The long noncoding RNA lncTCF7 promotes self-renewal of human liver cancer stem cells through activation of Wnt signaling. Cell Stem Cell. 2015;16(4):413–25. DOI:https://doi.org/10.1016/j.stem.2015.03.003.
36. Abdollahzadeh R, Daraei A, Mansoori Y, Sepahvand M, Amoli MM, Tavakkoly-Bazzaz J. Competing endogenous RNA (ceRNA) cross talk and language in ceRNA regulatory networks: A new look at hallmarks of breast cancer. J Cell Physiol. 2019;234(7):10080–100. DOI:https://doi.org/10.1002/jcp.27941.
37. Thompson AM, Martin KA, Rzucidlo EM. Resveratrol induces vascular smooth muscle cell differentiation through stimulation of SirT1 and AMPK. PLoS One. 2014;9(1):e85495. DOI:https://doi.org/10.1371/journal.pone.0085495.
38. Sun HM, Chen XL, Chen XJ, Liu J, Ma L, Wu HY, et al. PALLD Regulates Phagocytosis by Enabling Timely Actin Polymerization and Depolymerization. J Immunol. 2017;199(5):1817–26. DOI:https://doi.org/10.4049/jimmunol.1602018.
39. Yoshio T, Morita T, Kimura Y, Tsujii M, Hayashi N, Sobue K. Caldesmon suppresses cancer cell invasion by regulating podosome/invadopodium formation. FEBS Lett. 2007;581(20):3777–82. DOI:https://doi.org/10.1016/j.febslet.2007.06.073.
40. Zhengchun Liu X, Liu R, Cai M, Liu, Wang R. Identification of a tumor microenvironment-associated prognostic gene signature in bladder cancer by integrated bioinformatic analysis. Int J Clin Exp Pathol. 2021;14(5):551–66.
41. Branis J, Pataki C, Sporrer M, Gerum RC, Mainka A, Cermak V, et al. The role of focal adhesion anchoring domains of CAS in mechanotransduction. Sci Rep. 2017;7:46233. DOI:https://doi.org/10.1038/srep46233.
42. Paluch EK, Aspalter IM, Sixt M. Focal Adhesion-Independent Cell Migration. Annu Rev Cell Dev Biol. 2016;32:469–90. DOI:https://doi.org/10.1146/annurev-cellbio-111315-125341.
43. Zhou J, Kang X, An H, Lv Y, Liu X. The function and pathogenic mechanism of filamin A. Gene. 2021;784:145575. DOI:https://doi.org/10.1016/j.gene.2021.145575.
44. Ueda K, Fujiki K, Shirahige K, Gomez-Sanchez CE, Fujita T, Nangaku M, et al. Genome-wide analysis of murine renal distal convoluted tubular cells for the target genes of mineralocorticoid receptor. Biochem Biophys Res Commun. 2014;445(1):132–7. DOI:https://doi.org/10.1016/j.bbrc.2014.01.125.
45. Finlin BS, Gau CL, Murphy GA, Shao H, Kimel T, Seitz RS, et al. RERG is a novel ras-related, estrogen-regulated and growth-inhibitory gene in breast cancer. J Biol Chem. 2001;276(45):42259–67. DOI:https://doi.org/10.1074/jbc.M105888200.
46. Zhao W, Ma N, Wang S, Mo Y, Zhang Z, Huang G, et al. RERG suppresses cell proliferation, migration and angiogenesis through ERK/NF-kappaB signaling pathway in nasopharyngeal carcinoma. J Exp Clin Cancer Res. 2017;36(1):88. DOI:https://doi.org/10.1186/s13046-017-0554-9.

47. Zou H, Hu L, Li J, Zhan S, Cao K. Cloning and characterization of a novel small monomeric GTPase, RasL10B, with tumor suppressor potential. Biotechnol Lett. 2006;28(23):1901–8. DOI:https://doi.org/10.1007/s10529-006-9176-6.
48. Thillaivillalan Dhanaraman S, Singh RC, Killoran A, Singh X, Xu JM. Shifman, et al. RASSF effectors couple diverse RAS subfamily GTPases to the Hippo pathway. CELL BIOLOGY. 2020;13(635):1–15. DOI:10.1126/scisignal.abb4778. DOI.

Figures

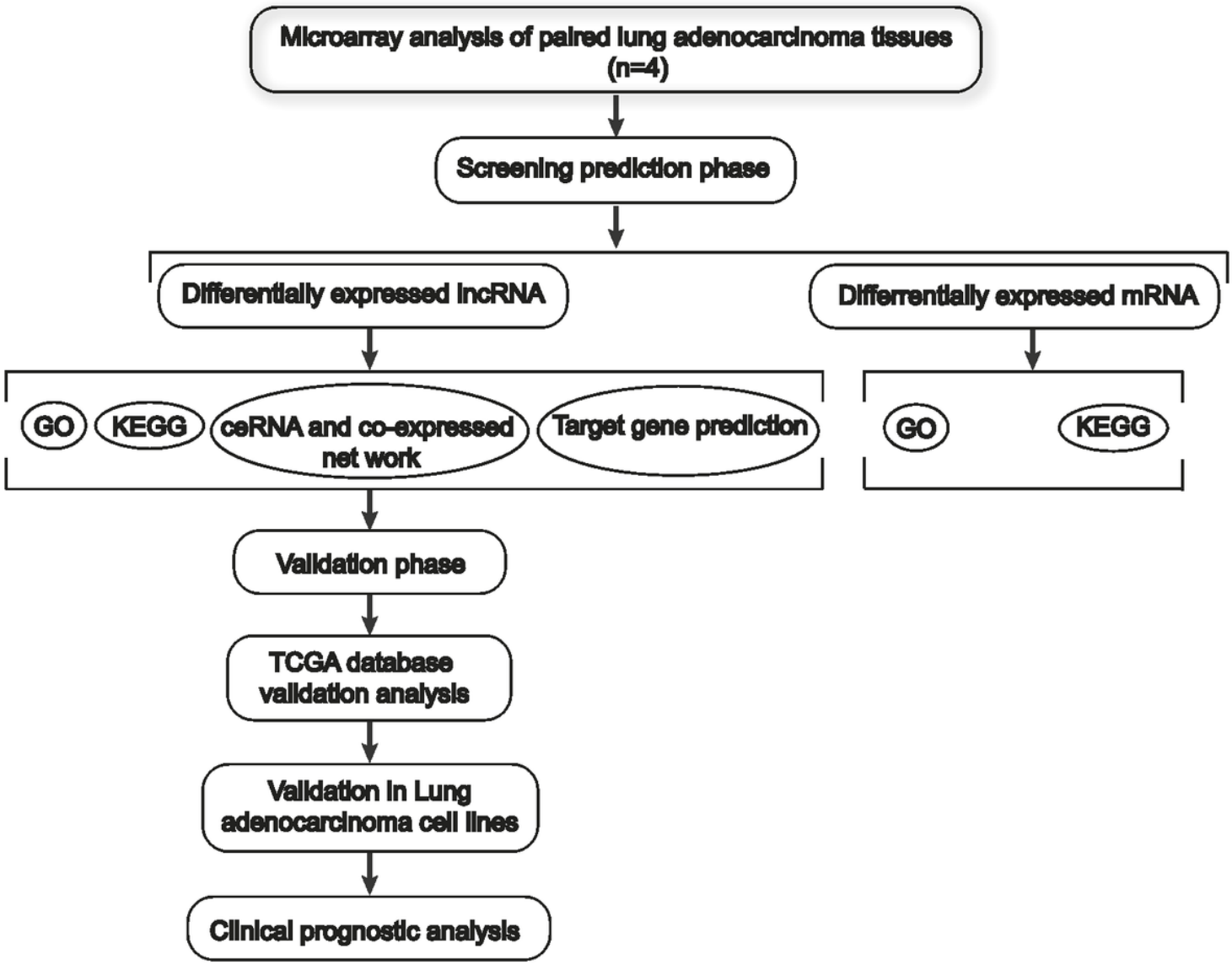

Figure 1

The flowchart of this study.

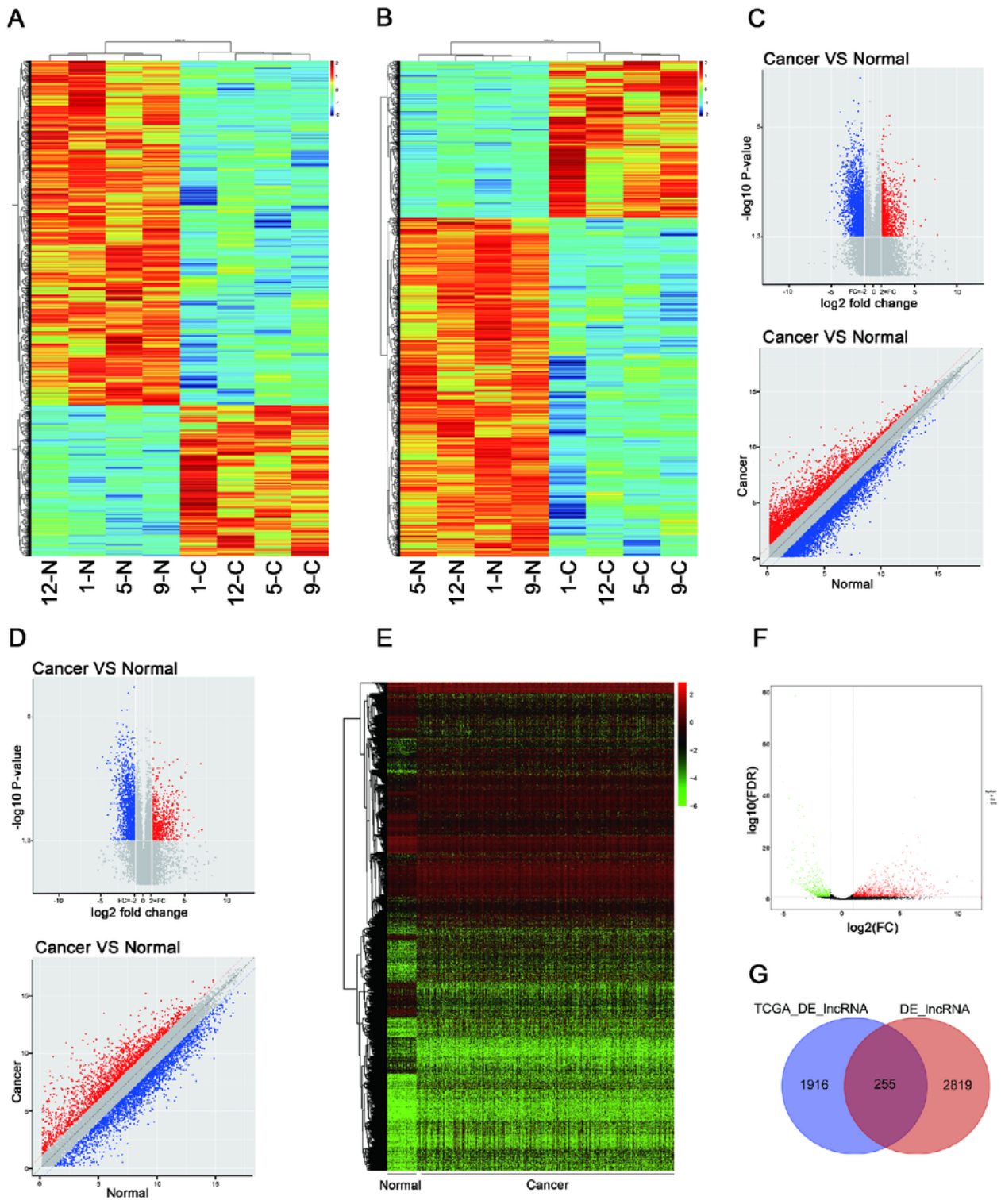

Figure 2

Screening of differentially expressed lncRNAs and mRNAs between LUAD tissues and normal tissues. (A) Heatmap of DE lncRNAs ;(B) Heatmap of DE mRNAs; the x-axis shows samples and the y-axis shows differentially expressed genes. Red and blue represent upregulated and downregulated differentially expressed genes, respectively. (C) Scatter and Volcano plots showing expression profiles of DE lncRNAs based on the expression values of lncRNAs detected by microarray (D) Scatter and Volcano plots

showing expression profiles of DE mRNAs based on the expression values of mRNAs detected by microarray; | FC | ≥2.0, P < 0.05. (E) The heatmap of DE lncRNAs 512 LUAD tissue samples and 59 adjacent tissue samples. Green and red represents downregulated and upregulated DE lncRNAs, respectively. (F) The volcano plot showed that a total of 1271 up-regulated lncRNAs and 645 down-regulated lncRNAs were screened out (| log2fc | > 1, P < 0.05). (G) the Venn diagram of TCGA DE lncRNAs and microarray DE lncRNAs.

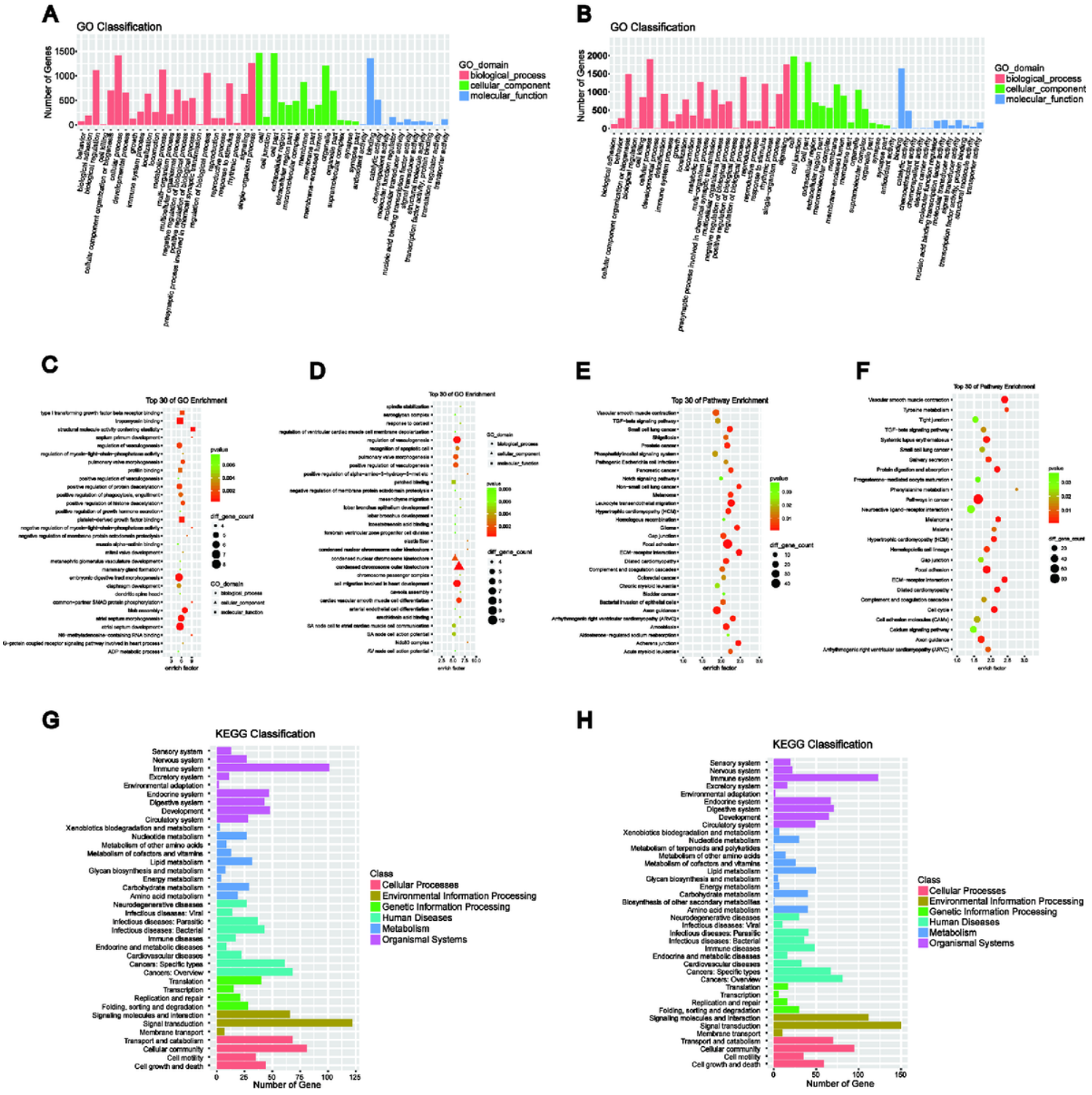

Figure 3

GO and KEGG enrichment analysis of DE lncRNAs and DE mRNAs. Barplot of top 30 GO classification enrich terms of DE lncRNAs (A) and DE mRNAs (B). Bubble Plot of top 30 GO level 2 enrich terms of DE lncRNAs (C) and DE mRNAs (D). Bubble Plot of top 30 KEGG pathway enrichment of DE lncRNAs (E) and DE mRNAs (F). (G, H) Barplot Plot of top 30 KEGG pathway classification of DE lncRNAs (G) and DE mRNAs (H). GeneRatio >=2, P <0.05.

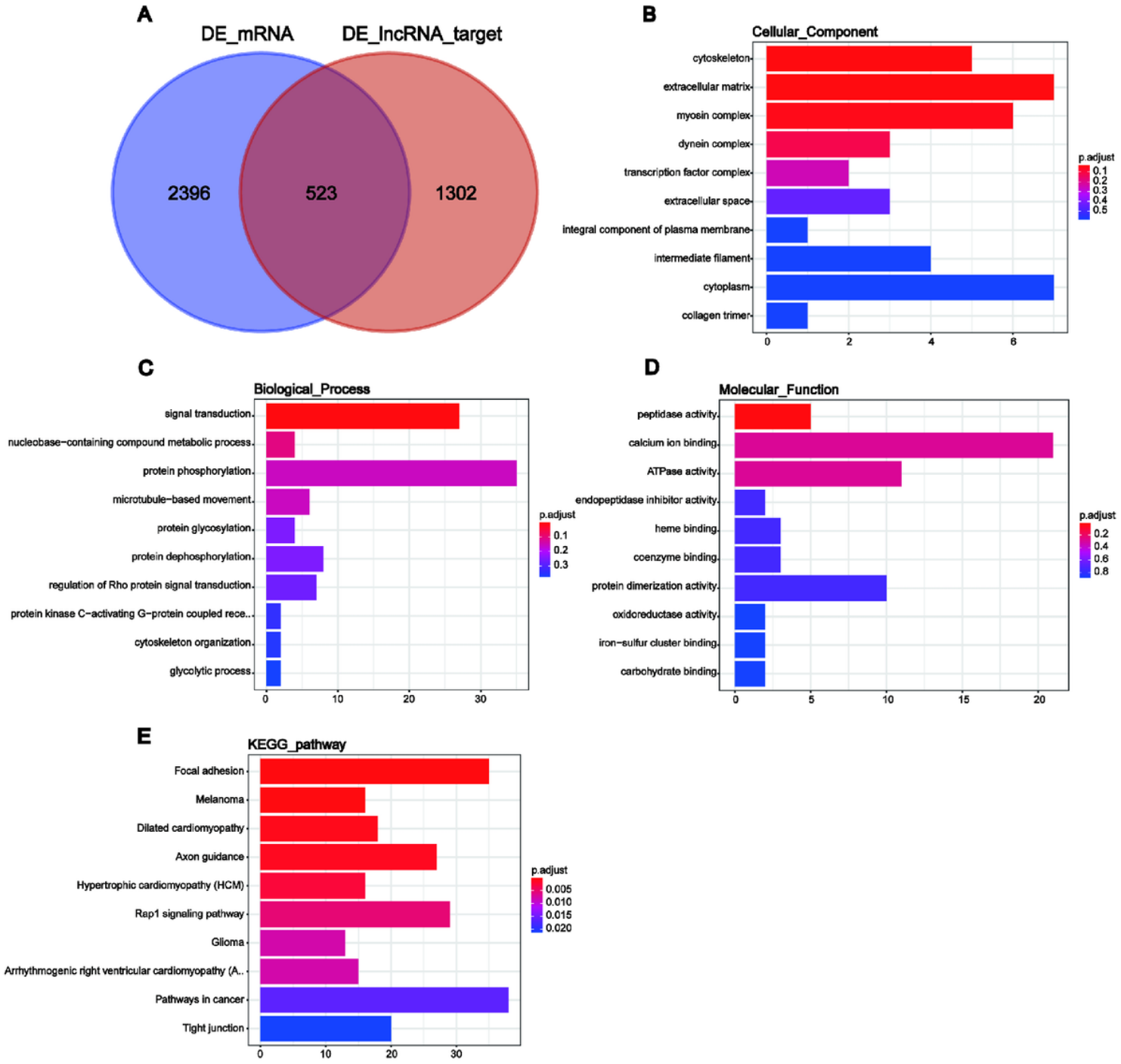

Figure 4

GO and KEGG enrichment analysis of the common genes of DE lncRNAs and DE mRNAs. (A) the Venn diagram of DE mRNAs and DE lncRNA target genes. (B) Cell component (CC). (C) Biological process (BP).

(D) Molecular function (MF). (D) KEGG Pathway. The y-axis shows significantly enriched categories of the targets, and the x-axis shows the enrichment scores of these terms. Barplot heigh denotes the number of genes located in the functional area.

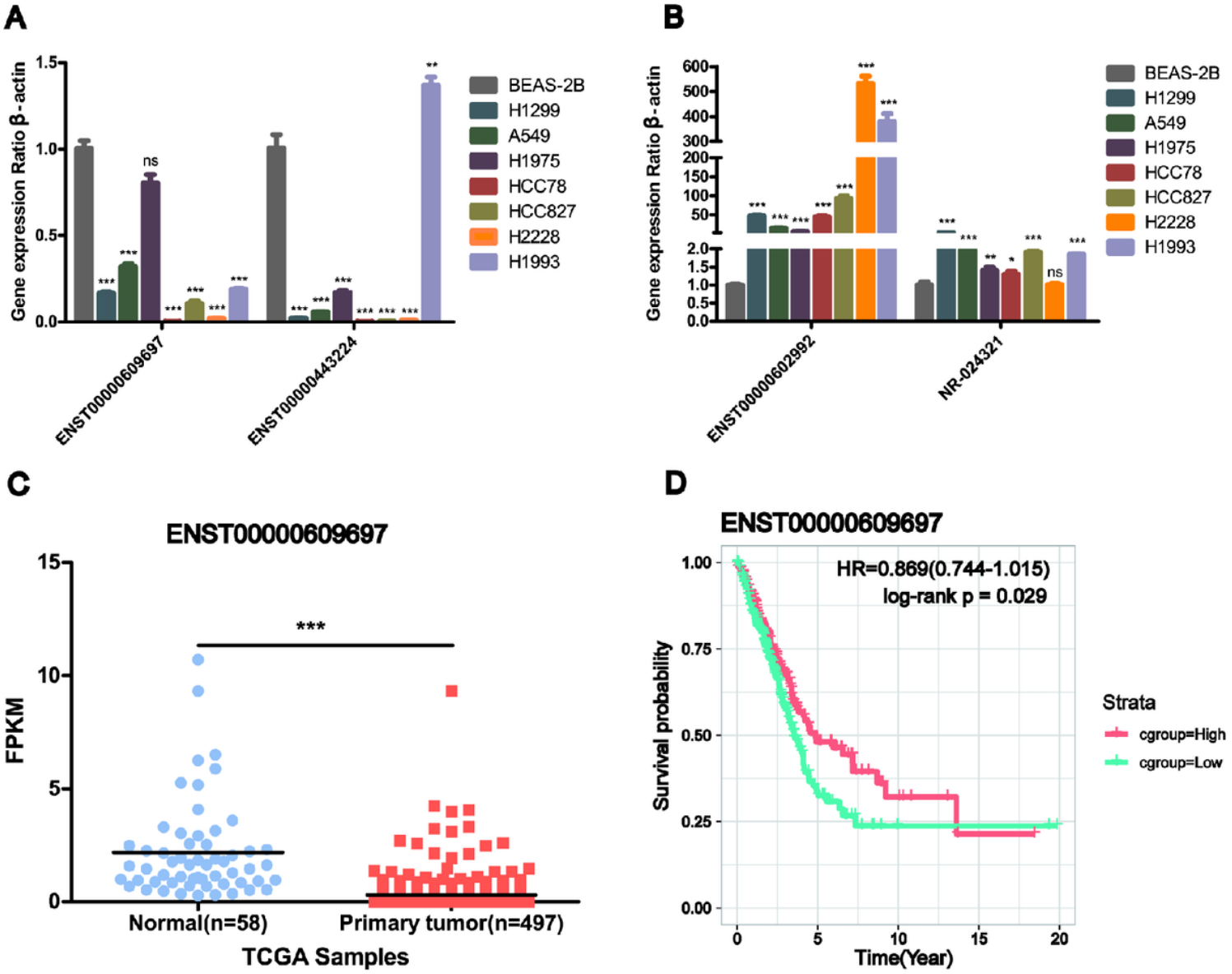

Figure 5

Validation of candidate lncRNAs. (A)To verify the expression level of down-regulation candidate lncRNAs in 7 LUAD cell lines and BEAS-2B via qRT-PCR. (B)To verify the expression level of up-regulation candidate lncRNAs in 7 LUAD cell lines and BEAS-2B via qRT-PCR. The data are presented as the mean ± standard error and three independent experiments. *p < 0.05; **p < 0.01; ***p < 0.001. (C) The relative expression of candidate DE lncRNA ENST00000609697 in TCGA dataset. (D)Kaplan–Meier (KM) survival analysis of candidate DE lncRNA ENST00000609697. x-axis: overall survival time (year); y-axis: survival rate. Green and red represents low- and high-group of the DE lncRNAs, respectively.

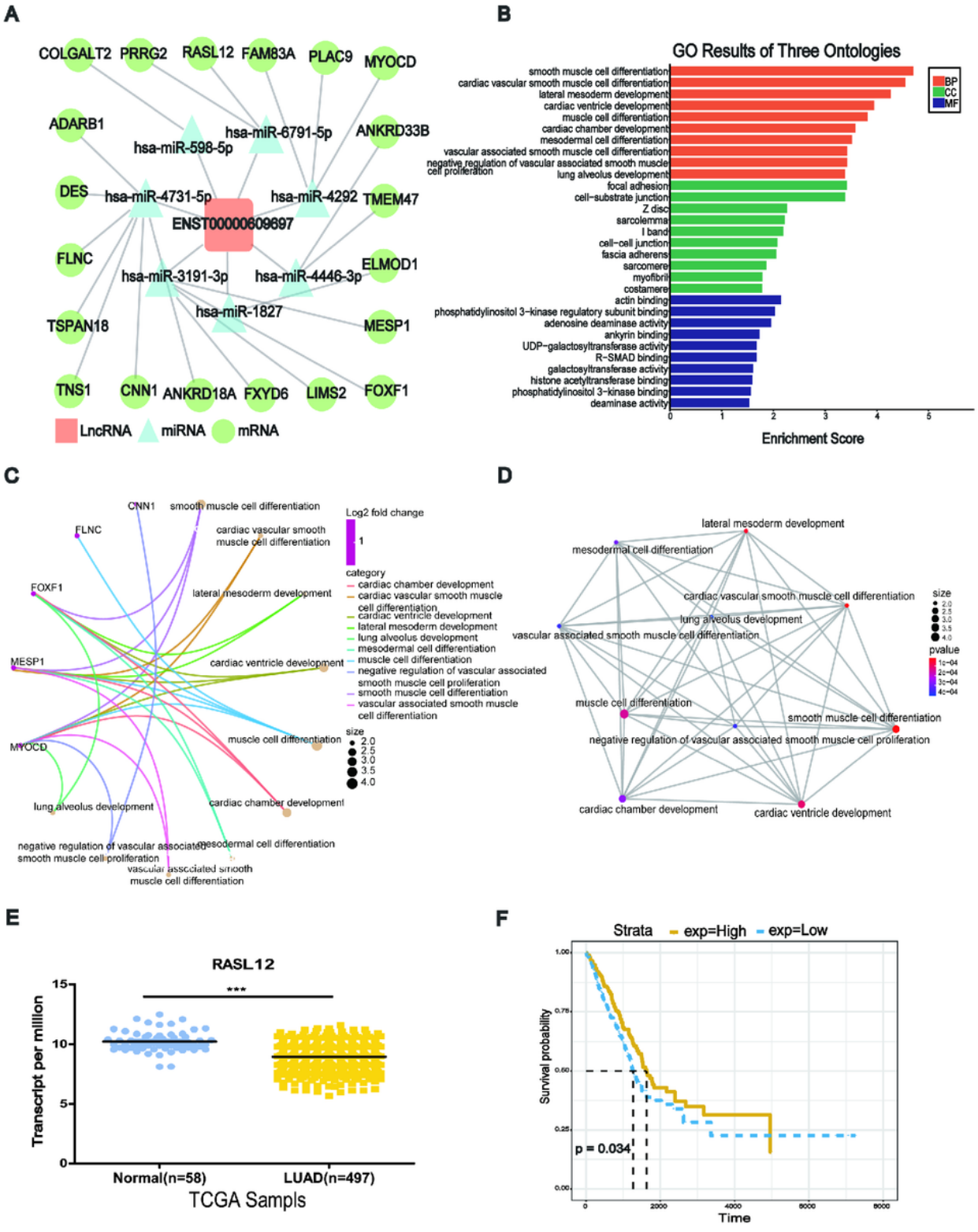

Figure 6

Target genes function annotation of ENST00000609697 ceRNA regulatory network. (A) ceRNA network of ENST00000609697. (B) Barplot of top 30 GO classification enrich terms of target genes, P<0.05. (C) BP cnetplot of target genes, P<0.001. (D) BP emaplot of target genes, P<0.001. (E) Relative expression of RASL12 in TCGA dataset, P<0.0001. (F) survival analysis of RASL12 in TCGA dataset, P=0.034.

Supplementary Files

This is a list of supplementary files associated with this preprint. Click to download.

- Supplyment1.pdf